Pressure-Induced Quenching of the Jahn-Teller Distortion and Insulator-to-Metal Transition in $LaMnO_3$

I. Loa,[1] P. Adler,[1] A. Grzechnik,[1] K. Syassen,[1] U. Schwarz,[2] M. Hanfland,[3] G. Kh. Rozenberg,[4] P. Gorodetsky,[4] and M. P. Pasternak[4]

[1]*Max-Planck-Institut für Festkörperforschung, Heisenbergstrasse 1, D-70569 Stuttgart, Germany*
[2]*Max-Planck-Institut für Chemische Physik fester Stoffe, Nöthnitzer Strasse 40, D-01187 Dresden, Germany*
[3]*European Synchrotron Radiation Facility, BP 220, F-38043 Grenoble, France*
[4]*School of Physics and Astronomy, Tel Aviv University, 69978 Tel Aviv, Israel*

(Received 2 April 2001; published 28 August 2001)

$LaMnO_3$ was studied by synchrotron x-ray diffraction, optical spectroscopies, and transport measurements under pressures up to 40 GPa. The cooperative Jahn-Teller (JT) distortion is continuously reduced with increasing pressure. There is strong indication that the JT effect and the concomitant orbital order are completely suppressed above 18 GPa. The system, however, retains its insulating state to ~32 GPa, where it undergoes a bandwidth-driven insulator-metal transition. Delocalization of electron states, which suppresses the JT effect but is insufficient to make the system metallic, appears to be a key feature of $LaMnO_3$ at 20–30 GPa.

DOI: 10.1103/PhysRevLett.87.125501 PACS numbers: 61.50.Ks, 71.30.+h, 71.38.–k, 78.30.–j

Perovskite-type manganites have recently received renewed interest after the observation of a "colossal" negative magnetoresistance (CMR) effect in $La_{1-x}Ca_xMnO_3$ [1] and related materials. Correlated magnetic and metal-insulator transitions are observed as a function of temperature, magnetic field, and doping along with charge and orbital ordering/disordering phenomena (for recent reviews, see [2,3]). The complex electronic properties of doped manganites originate from an intimate interplay of lattice and electronic degrees of freedom. This is also the case for the undoped parent compound, $LaMnO_3$. At ambient conditions $LaMnO_3$ is an insulator with orthorhombic perovskite structure (space group *Pnma* [4]). Alternating long and short Mn-O2 distances in the *ac* plane of the structure are a sign of orbital ordering which arises from a cooperative Jahn-Teller (JT) distortion. The latter removes the degeneracy of the e_g orbitals in the $t_{2g}^3 e_g^1$ electron configuration of the Mn^{3+} ions and stabilizes the $3d_{3z^2-r^2}$ with respect to the $3d_{x^2-y^2}$ orbitals. It is the origin of *A*-type antiferromagnetism below $T_N \approx 140$ K [5].

There has been intense discussion about the primary cause of the insulating ground state of $LaMnO_3$ (see, for example, Refs. [6,7]). In one interpretation $LaMnO_3$ is regarded, like many insulating transition-metal oxides, as a Mott-type (or charge-transfer) insulator, i.e., the electrical properties are dominated by electron-electron interactions leading to a localization of the e_g conduction electrons. On the other hand, Millis *et al.* concluded that the insulating behavior of the paramagnetic phase cannot be explained by a purely electronic model [6]. Strong Jahn-Teller electron-phonon coupling was proposed as the crucial component which localizes the e_g electrons as polarons.

High pressure is a means to tune the interplay between lattice and electronic degrees of freedom in $LaMnO_3$. We have studied the effect of hydrostatic pressure on the structural, vibrational, optical, and electronic properties of $LaMnO_3$ by angle-dispersive synchrotron x-ray powder diffraction, Raman spectroscopy, optical reflectivity, and electrical resistance measurements. Our data reveal that the cooperative Jahn-Teller distortion of $LaMnO_3$ is continuously reduced with increasing pressure. The JT effect and the concomitant orbital ordering appear to be completely suppressed above 18 GPa. Nevertheless, the compound remains in an insulating state up to much higher pressures of 32 GPa, where an insulator-to-metal transition occurs. The observation of an insulating state with suppressed JT effect supports the view that the JT distortion is not crucial to the stabilization of an insulating ground state in $LaMnO_3$.

$LaMnO_3$ was prepared from a stoichiometric mixture of La_2O_3 and Mn_2O_3 which was prefired in air at 1300 °C, pressed into pellets, and fired again at 1300 °C. Finally, the sample was heated at 700 °C in a gas flow containing 95% Ar and 5% H_2. The lattice parameters and Mn-O distances of our sample at ambient conditions are in good agreement with the values reported for stoichiometric $LaMnO_{3.00}$ [4].

The structural properties of $LaMnO_3$ under pressure were studied up to 40 GPa by monochromatic ($\lambda =$ 45.09 pm) x-ray powder diffraction at the European Synchrotron Radiation Facility (ESRF Grenoble, beam line ID9). Diffraction patterns were recorded on image plates and then integrated [8] to yield intensity vs 2θ diagrams. A diamond anvil cell (DAC) was used for pressure generation with nitrogen as a pressure medium to provide nearly hydrostatic conditions. Raman spectra of $LaMnO_3$ up to 16 GPa (DAC, methanol/ethanol pressure medium) were recorded using an Ar-ion laser (515 nm) and a triple-grating spectrometer with a CCD detector. Optical reflectivity spectra of $LaMnO_3$ in the energy range 0.6–4.0 eV were measured at pressures up to 38 GPa using

a micro-optical setup and sample loading procedures (KCl pressure medium) described in Ref. [9]. All of the above experiments were performed at $T = 300$ K. Four-probe dc resistance measurements were carried out with 5–7 μm thick Pt foil electrodes as a function of temperature and pressure [10]. The sample/metal-gasket cavity was coated with an insulating mixture of Al_2O_3/NaCl combined with epoxy. No pressure-transmitting medium was used. In all experiments pressures were measured with the ruby luminescence method [11].

Typical diffraction patterns of $LaMnO_3$ are shown in Fig. 1(a) for the pressure range 0–40 GPa. Up to 11 GPa the diffraction patterns were suitable for Rietveld refinements [12] yielding the lattice parameters and the atomic positions. Figure 1(b) shows the result of a refinement for a pressure of 5.9 GPa. Above 11 GPa, lattice parameters were determined from full-profile fits with the atomic positions fixed to the 11-GPa values (space group *Pnma*).

Figure 2(a) illustrates the pressure dependence of the lattice parameters. The *b*-axis data are normalized by a factor of $2^{-1/2}$ corresponding to a pseudocubic representation of the lattice. Up to 15–20 GPa, the compression is anisotropic with the soft direction along the *a* axis. Its initial compressibility is ~4 times larger than those of the *b* and *c* axes. The compressibilities along the *c* and *a* directions change markedly at ~7 and ~18 GPa, respectively. $LaMnO_3$ remains orthorhombic to at least 40 GPa.

From the lattice parameter data we obtain the pressure dependence of the unit-cell volume shown in Fig. 2(b). The $V(P)$ data are well described by the Murnaghan equation [13] which yields the bulk modulus B_0 and its pressure derivative B' at zero pressure. The large value of $B' = 8.5 \pm 0.4$ (compared to typical values of $B' \approx 4$–6 for crystals with nearly isotropic compression) reflects the pronounced anisotropic compressibility.

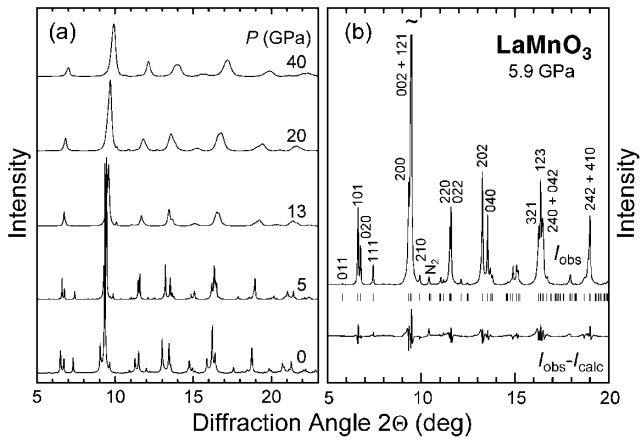

FIG. 1. (a) X-ray powder diffraction patterns of $LaMnO_3$ at various pressures ($T = 298$ K). (b) Diffraction pattern at 5.9 GPa and difference between the observed and calculated profile. Marks show the calculated peak positions. The reflection marked "N_2" is due to solid nitrogen.

Figure 2(c) shows the free positional parameters *x* and *z* of the La ions as a function of pressure. The *x* parameter decreases continuously and becomes zero near 12 GPa. This is also evidenced directly by the decreasing intensity of the (111) reflection [cf. Fig. 1 and inset of Fig. 2(c)]. The fact that this reflection does not reappear at higher pressures implies that the La ions remain located at $x = 0$ (and $x = 1/2$) at pressures above 12 GPa. The structural data further indicate that the relative compression of the distorted MnO_6 octahedra is larger than that of the unit cell [inset in Fig. 2(b)]. This implies that the octahedral tilting *decreases* with increasing pressure, consistent with the shift of the La ion. Mizokawa *et al.* concluded that at ambient pressure the shift of the La ion, driven by the $GdFeO_3$-type distortion, is essential to stabilize the orbital ordering [14]. The observed reversal of this shift thus suggests a *destabilization of the orbital order* at high pressures.

The three Mn-O distances of the distorted MnO_6 octahedra decrease under pressure [Fig. 2(d)]. This effect is most

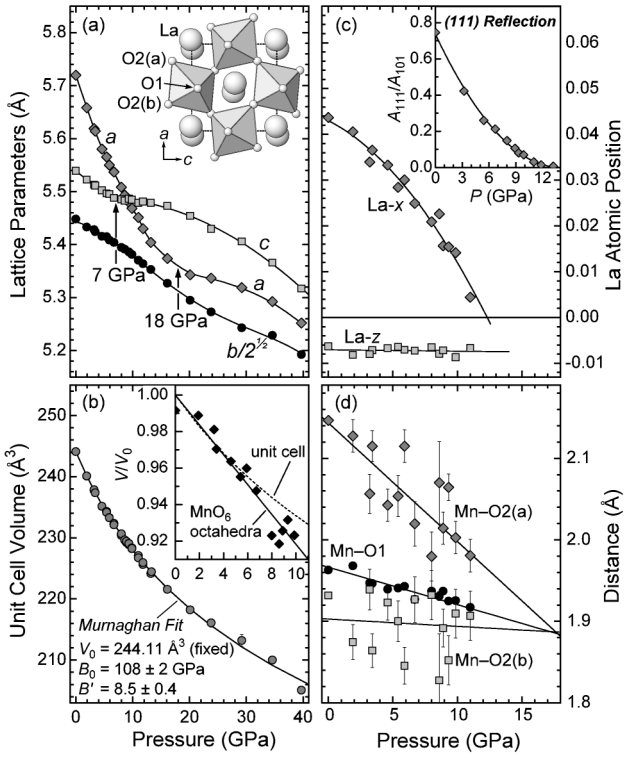

FIG. 2. (a) Lattice parameters of $LaMnO_3$ at ambient temperature as a function of pressure. There are marked changes of the *a* and *c* axis compressibility at 7 and 18 GPa, respectively. The inset shows the crystal structure of $LaMnO_3$ at ambient conditions (space group *Pnma*). (b) Unit-cell volume versus pressure. The inset depicts the volume of the MnO_6 octahedra up to 10 GPa. (c) Atomic coordinates of La as a function of pressure ($y_{La} = 1/4$). The inset shows the evolution of the intensity of the (111) reflection normalized to the (101) peak. (d) Mn-O distances of the distorted MnO_6 octahedra as a function of pressure.

pronounced for the Mn-O2 (a) distance which relates to the large a axis compressibility at low pressures. Extrapolation of the data suggests all Mn-O bond lengths become nearly equal around 18 GPa, which coincides with the occurrence of the a axis compression anomaly. This equalization of the Mn-O distances means that the *cooperative Jahn-Teller effect is reduced with increasing pressure,* a process which appears to be completed near 18 GPa.

Raman spectroscopy (Fig. 3) shows that the structural changes are more complex than indicated by the x-ray data which reflect the average long-range order. The B_{2g} Raman peak (1) at 610 cm^{-1} (in-phase O2 stretching mode [15]) shifts towards higher energy and loses intensity with increasing pressure. From the extrapolation of the intensity-versus-pressure data, it is expected to vanish near 18 GPa. A new peak (2) starts to appear near 7 GPa, approximately 45 cm^{-1} higher in energy than peak (1). The intensity redistribution from the O2 stretching mode (1) to the new higher-energy peak (2) shows that a sluggish transition occurs that is not evident from the x-ray data.

The pressure range 7–18 GPa, in which the Raman intensity redistribution takes place, coincides with that marked by the anomalies of the c and a lattice parameters. Together with the absence of distinct changes of atomic positions around 7 GPa, these findings suggest the following scenario: After compression of the sample up to 7 GPa, domains start to form. In these domains the MnO_6 octahedra adopt a less distorted, contracted shape which results in the new *higher-energy* Raman peak. The lattice parameters of the two phases are very similar since no peak splitting is observed in the diffraction experiment. This is easily understood as the octahedral contraction can be compensated (with regard to the lattice parameters) by a change of the octahedral tilting.

The combined x-ray and Raman data show that the cooperative Jahn-Teller effect in $LaMnO_3$ is reduced by application of hydrostatic pressure. There is a strong indication that the Jahn-Teller distortion is completely suppressed at 18 GPa.

A pressure-induced insulator–metal transition takes place at pressures much higher than required to suppress the Jahn-Teller effect. It occurs at ~32 GPa as evidenced by optical reflectivity and electrical resistance measurements (Fig. 4). The broad spectral feature around 2 eV [Fig. 4(a)] corresponds to an optical transition and a related gap near 1 eV, consistent with the insulating nature of $LaMnO_3$ at ambient pressure. Up to 18 GPa—i.e., in the pressure range where the suppression of the Jahn-Teller distortion occurs—only small changes of the optical response are observed. Above 30 GPa, the near-infrared reflectivity increases strongly [inset of Fig. 4(a)] indicating an insulator-to-metal transition in agreement with the electrical resistance experiments. At 32 GPa these show a change in sign of the resistance derivative, dR/dT, namely from semiconductor to metal behavior [Fig. 4(b)]. In addition, a sharp drop of the ambient-temperature resistance occurs at the same pressure [inset of Fig. 4(b)]. The system retains a rather high resistance, i.e., it is a "poor" metal.

Our results suggest the existence of three distinct regimes: (i) an insulating one with JT distortion and orbital ordering [<18 GPa], (ii) an intermediate one with suppressed JT distortion and no orbital ordering, but still insulating [18–32 GPa], and (iii) a metallic phase without JT effect [>32 GPa]. For a certain range of pressures undoped $LaMnO_3$ thus exists in an insulating state which is not caused by the JT effect. This supports the view that $LaMnO_3$ basically is a Mott (or charge-transfer) insulator.

The observed decrease of the Mn-O distances under pressure and the decreasing octahedral tilting both enhance

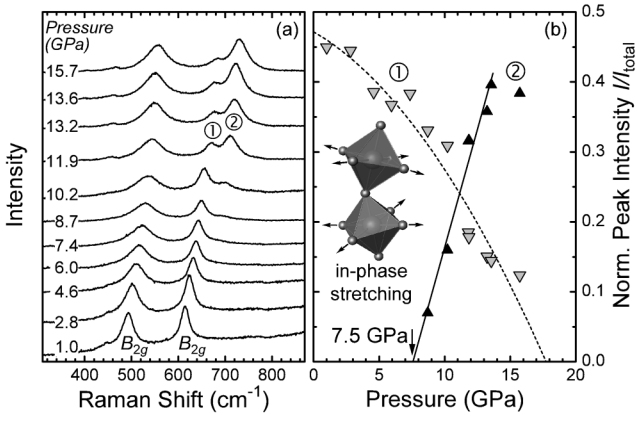

FIG. 3. (a) Raman spectra of $LaMnO_3$ at 300 K in the pressure range 0–16 GPa. (b) Intensities versus pressure of the B_{2g} mode (1) at 610 cm^{-1} that was assigned to the in-phase O2 stretching vibration and of the peak (2) appearing above 7 GPa.

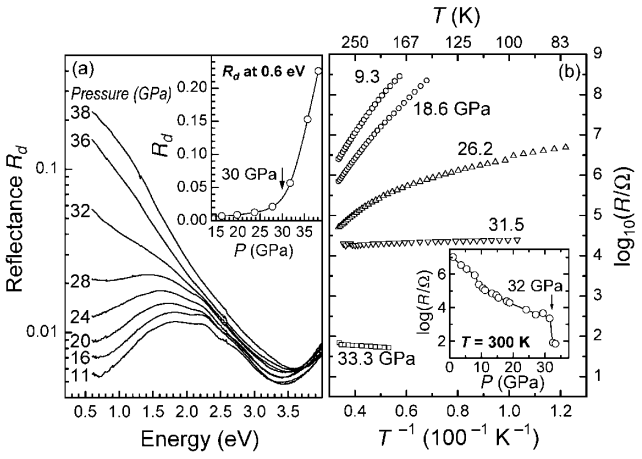

FIG. 4. (a) Optical reflectivity spectra of $LaMnO_3$ at T = 300 K as a function of pressure. R_d denotes the absolute reflectivity of the interface between sample and diamond of the pressure-generating DAC. (Note the logarithmic scale.) The inset shows the pressure dependence of the near-infrared reflectivity at 0.6 eV. (b) Temperature dependence of the resistance $\log_{10}(R/\Omega)$ for selected pressures up to 33 GPa. The inset depicts the pressure dependence of the resistance at T = 300 K.

the Mn-O-Mn interactions and hence the bandwidth arising from the e_g orbitals. In the intermediate insulating state the e_g electrons are already sufficiently delocalized to suppress the JT effect, but still not itinerant enough to make the system metallic. The energetics in such an intermediate regime have been discussed by Goodenough [16]. It cannot be excluded from our data that the stabilization of this insulating state involves other instabilities, e.g., a charge-density wave formation similar to that observed in the isoelectronic ($t_{2g}^3 e_g^1$) Fe^{4+} oxide $CaFeO_3$ [17]. In contrast to the CMR materials, the insulator-metal transition in $LaMnO_3$ is driven by an increased bandwidth and not by chemical doping.

The notion of delocalization of e_g (or t_{2g}) electrons without metallization seems also of relevance for other transition metal oxides with Jahn-Teller electron configurations, e.g., Fe^{4+} oxides [18], rare earth nickelates ($t_{2g}^6 e_g^1$ Ni^{3+} ions) [19], and $LaTiO_3$ (t_{2g}^1 Ti^{3+}ions) [20]. At ambient pressure many of these materials are close to the insulator-metal borderline and some reveal insulating states without signs of orbital ordering. However, the noncontinuous variation of the structural and electronic properties across the series of these oxides with varying chemical composition has hindered a clear recognition of their correlations.

The pressure-induced changes described above are expected to alter the magnetic properties of $LaMnO_3$. The suppression of the orbital order may lead to a collapse of the *A*-type antiferromagnetic order observed at low temperature. The increasing delocalization of the e_g electrons which show Hund's rule coupling to the more localized t_{2g} electrons, possibly favors magnetic structures with enhanced ferromagnetic interactions (e.g., a spiral or ferromagnetic spin arrangement).

In conclusion, we have studied the structural changes of undoped $LaMnO_3$ under high hydrostatic pressure and their relation to the electronic properties. The pronounced cooperative Jahn-Teller distortion and the $GdFeO_3$-type distortion (octahedral tilting) decrease with increasing pressure. We infer that the JT effect and the concomitant orbital order are completely suppressed at 18 GPa. On the other hand, the system remains insulating to $\sim$32 GPa where it undergoes a bandwidth-driven insulator-metal transition. The observation of an insulating state with suppressed JT effect supports the view that $LaMnO_3$ is a Mott (or charge-transfer) insulator, the JT distortion rather being a consequence of the localization of the e_g electrons than its origin. Delocalization of electron states which suppresses the JT effect, but is too weak to make the system metallic, appears to be a key feature of insulating transition metal oxides with quenched JT distortion.

[1] S. Jin *et al.,* Science **264**, 413 (1994).
[2] A. P. Ramirez, J. Phys. Condens. Matter **9**, 8171 (1997).
[3] J. M. D. Coey, M. Viret, and S. von Molnár, Adv. Phys. **48**, 167 (1999).
[4] N. Sakai, H. Fjellvåg, and B. Lebech, Acta Chem. Scand. **51**, 904 (1997); M. R. Ibarra *et al.,* Phys. Rev. B **56**, 8902 (1997); J. Rodríguez-Carvajal *et al.,* Phys. Rev. B **57**, 3189 (1998).
[5] E. O. Wollan and W. C. Koehler, Phys. Rev. **100**, 545 (1955); J. B. Goodenough, Phys. Rev. **100**, 564 (1955); B. C. Hauback, H. Fjellvåg, and N. Sakai, J. Solid State Chem. **124**, 43 (1996); D. D. Sarma *et al.,* Phys. Rev. Lett. **75**, 1126 (1995).
[6] A. J. Millis, P. B. Littlewood, and B. I. Shraiman, Phys. Rev. Lett. **74**, 5144 (1995); A. J. Millis, R. Mueller, and B. I. Shraiman, Phys. Rev. B **54**, 5405 (1996).
[7] C. M. Varma, Phys. Rev. B **54**, 7328 (1996); L. F. Feiner and A. M. Oleś, Phys. Rev. B **59**, 3295 (1999); N. Furukawa, J. Phys. Soc. Jpn. **63**, 3214 (1994).
[8] A. Hammersley, computer program FIT2D, ESRF, Grenoble, 1998.
[9] A. R. Goñi and K. Syassen, in *High Pressure in Semiconductor Physics I,* edited by T. Suski and W. Paul (Academic, New York, 1998), p. 248.
[10] G. K. Rozenberg *et al.,* Phys. Rev. B **53**, 6482 (1996).
[11] H. K. Mao, J. Xu, and P. M. Bell, J. Geophys. Res. **91**, 4673 (1986).
[12] A. C. Larson and R. B. von Dreele, Report No. LAUR 86-748, Los Alamos National Laboratory, New Mexico, 1986.
[13] F. D. Murnaghan, Proc. Natl. Acad. Sci. U.S.A. **30**, 244 (1944).
[14] T. Mizokawa, D. I. Khomskii, and G. A. Sawatzky, Phys. Rev. B **60**, 7309 (1999).
[15] M. N. Iliev *et al.,* Phys. Rev. B **57**, 2872 (1998).
[16] J. L. Goodenough, Prog. Solid State Chem. **5**, 145 (1971).
[17] P. M. Woodward *et al.,* Phys. Rev. B **62**, 844 (2000); T. Takeda *et al.,* Solid State Sci. **2**, 673 (2000).
[18] P. Adler *et al.,* Phys. Rev. B **60**, 4609 (1999).
[19] M. Imada, A. Fujimori, and Y. Tokura, Rev. Mod. Phys. **70**, 1039 (1998); J. B. Torrance *et al.,* Phys. Rev. B **45**, 8209 (1992).
[20] B. Keimer *et al.,* Phys. Rev. Lett. **85**, 3946 (2000); G. Khaliullin and S. Maekawa, Phys. Rev. Lett. **85**, 3950 (2000).